International Journal of Medical Microbiology 314 (2024) 151598

Contents lists available at ScienceDirect

International Journal of Medical Microbiology

journal homepage: www.elsevier.com/locate/ijmm

Different populations of A(H1N1)pdm09 viruses in a patient with hemolytic-uremic syndrome

Yuguang Fu [a,b,1], Marianne Wedde [c,1], Sigrun Smola [d], Djin-Ye Oh [c], Thorsten Pfuhl [d], Jürgen Rissland [d], Michael Zemlin [e], Fidelis A. Flockerzi [f], Rainer M. Bohle [f], Andrea Thürmer [g], Susanne Duwe [c], Barbara Biere [c], Janine Reiche [c], Brunhilde Schweiger [c], Christin Mache [c], Thorsten Wolff [c], Georg Herrler [b], Ralf Dürrwald [c,*,1]

[a] State Key Laboratory of Veterinary Etiological Biology, Lanzhou Veterinary Research Institute, Chinese Academy of Agricultural Sciences, Lanzhou 730046, China
[b] Institute of Virology, University of Veterinary Medicine Hannover, Foundation, Hannover 30559, Germany
[c] Influenza and other Respiratory Viruses, Department of Infectious Diseases, Unit 17, Influenza and other Respratory Viruses, Robert Koch Institute, Berlin 13353, Germany
[d] Institute of Virology, Saarland University Medical Center, Homburg, Saar 66421, Germany
[e] Department for General Pediatrics and Neonatology, Saarland University Medical Center, Homburg, Saar 66421, Germany
[f] Institute of Pathology, Saarland University Medical Center, Homburg, Saar 66421, Germany
[g] Department Methods Development and Research Infrastructure, Robert Koch Institute, Berlin 13353, Germany

ARTICLE INFO

Keywords:
A(H1N1)pdm09 virus
Fatal influenza
S263S/F (HA1) and H456H/Y (PB1) mutations

ABSTRACT

Respiratory viral infections may have different impacts ranging from infection without symptoms to severe disease or even death though the reasons are not well characterized.

A patient (age group 5–15 years) displaying symptoms of hemolytic uremic syndrome died one day after hospitalization. qPCR, next generation sequencing, virus isolation, antigenic characterization, resistance analysis was performed and virus replication kinetics in well-differentiated airway cells were determined.

Autopsy revealed hemorrhagic pneumonia as major pathological manifestation. Lung samples harbored a large population of A(H1N1)pdm09 viruses with the polymorphism H456H/Y in PB1 polymerase. The H456H/Y viruses replicated much faster to high viral titers than upper respiratory tract viruses in vitro. H456H/Y-infected air-liquid interface cultures of differentiated airway epithelial cells did reflect a more pronounced loss of ciliated cells. A different pattern of virus quasispecies was found in the upper airway samples where substitution S263S/F (HA1) was observed.

The data support the notion that viral quasispecies had evolved locally in the lung to support high replicative fitness. This change may have initiated further pathogenic processes leading to rapid dissemination of inflammatory mediators followed by development of hemorrhagic lung lesions and fatal outcome.

1. Introduction

In 2009, a new influenza A virus emerged in Mexico and spread quickly through the global human population, thereby causing the first influenza pandemic of the 21st century (Mena et al., 2016). The A(H1N1)pdm09 virus caused severe influenza and increased hospitalizations in children, pregnant women and young adults with underlying risks like cardiac disease, obesity or chronic diseases (Girard et al., 2010). The severity of pandemic influenza was particularly high in children less than 14 years of age (Dawood et al., 2012) and remained unchanged through the first post pandemic season (Altmann et al., 2012). In the following seasons up until the present time, severe and sometimes fatal influenza courses have been observed occasionally in individual children (Skowronski et al., 2019; Streng et al., 2015).

The sudden onset of illness and a predominance of nonrespiratory symptoms can complicate the diagnosis of A(H1N1)pdm09 virus-infected children and may hinder rapid treatment. The application of novel techniques such as next generation sequencing (NGS) enables the

* Correspondence to: Robert Koch Institute, Unit 17: Influenza and Other Respiratory Viruses, National Influenza Center, Seestr. 10, 13353 Berlin, Germany.
E-mail address: DuerrwaldR@rki.de (R. Dürrwald).
[1] These authors contributed equally.

https://doi.org/10.1016/j.ijmm.2024.151598
Received 3 August 2023; Received in revised form 3 January 2024; Accepted 9 January 2024
Available online 11 January 2024

investigation of respiratory viral subpopulations in extraordinary depth in order to elucidate clinical differences in pathogenesis. However, data on viral populations from the entire respiratory tract are still scarce for severe A(H1N1)pdm09 influenza cases. Here we investigated respiratory tract samples from a fatal case of A(H1N1)pdm09 influenza associated with an unusual clinical course, including a presentation with predominantly renal manifestations prior to the development of acute respiratory distress syndrome in the final stage.

2. Material and methods

2.1. Samples

Oropharyngeal swab, blood and stool samples had been taken shortly after admission of a patient displaying gastrointestinal symptoms including emesis and later acute respiratory distress syndrome (in the season 2017/18). The patient died 13 h after admission. At autopsy, specimens from lower (lung, trachea, larynx) and upper respiratory tract (pharyngeal swabs) were obtained.

2.2. Ethics statement

The publication of the fatal case was approved by the Ethical Board of Ärztekammer des Saarlandes (reference 283/21). All data analyses were done anonymously.

Further samples were investigated for purposes of influenza surveillance in Germany. These investigations were approved by Charité Universitätsmedizin Berlin Ethical Board (reference EA2/126/11 and EA2/218/19). This surveillance is covered by German legislation (§13, §14, Protection against Infection Act).

2.3. Cells and viruses

Influenza viruses were isolated by inoculation of MDCK-SIAT cells (Matrosovich et al., 2003) as described recently (Rath et al., 2017). For comparative analyses, we used viruses of the last seasons, which were selected from the German National Influenza Centre's specimen repository.

2.4. qPCR

RNA was extracted using the NucliSens® easyMAG™ (bioMérieux, Nürtingen, Germany) from 400 µl sample material (throat swab) or ~25 mg biopsy material, homogenised in 500 µl NaCl (0,9 %) by a TissueLyser II™ (Qiagen, Hilden, Germany) according to the manufacturer`s instructions. 10 µl eluate was used to perform multiplex (RT-) PCRs using the FTD Respiratory pathogens 21 Assay (Fast Track Diagnostics, Luxembourg) according to the manufacturer`s instructions on LC480II real-time PCR thermal cyclers (Roche). Independent RNA extraction was performed from 200 µl sample material (homogenized, if applicable) using the MagNaPure96 DNA and Viral NA Small Volume Kit (Roche) and eluted in 50 µl elution buffer. 12.5 µl of extracted RNA were subjected to cDNA synthesis in a total reaction volume of 20 µl, applying random hexamer primers and 200 U M-MLV Reverse Transcriptase (Invitrogen). Synthesised cDNA was diluted 1:1 with H_2O to a total volume of 40 µl to allow robotic pipetting of 384-well PCR plates.

qPCR was carried out on LC480II real-time PCR thermal cyclers (Roche) in a total reaction volume of 15 µl. The reaction contained 1x PCR buffer, 4 mmol/L $MgCl_2$, 1 mmol/L dNTP (ThermoFisher) with dUTP (GE Healthcare), 600 ng BSA (ThermoFisher), 1 U Platinum Taq Polymerase (ThermoFisher), variable concentrations of primers and probes (available on request), and 5 µl of the prediluted cDNA. After 5 min at 95 °C for Taq DNA polymerase activation, a total of 45 cycles consisting of denaturation at 95 °C for 15 s and annealing at 60 °C for 30 s were performed. After the run, data were analysed using the LightCycler software version 1.5.1.62.

2.5. Sequencing

Upper respiratory tract specimens collected in the seasons 2017/18 (n = 57), 2018/19 (n = 65), 2019/20 (n = 141) and 2022/23 (n = 55) as well as viruses recovered from clinical samples in MDCK-SIAT cells were analyzed by cycle sequencing and next generation sequencing (NGS).

2.5.1. Sequence analysis pre-treatment - RNA extraction and one step PCR

Viral RNA was extracted (patient material or 1:1000 diluted cell culture supernatant from infected MDCK-SIAT cells) using ReliaPrep™ Cell Mini Kit (Promega). Using viral RNA (14 µl) and SuperScript™ III One-Step RT-PCR System with Platinum™ Taq High Fidelity DNA Polymerase (Invitrogen) multisegment reverse transcription-PCR were done according to Zhou et al. (2009).

2.5.2. Nested PCR for HA and NA gene amplification

Prior cycle-sequencing the hemagglutinin (HA) and neuraminidase (NA) genes of A(H1N1)pdm09 viruses were amplified performing nested PCRs (primer sequences on request) using an Eppendorf thermal cycler (Eppendorf). Each PCR was performed using 1 µl One-Step RT-PCR product (2.5 µl for CT values ≥30, previously determined by real-time PCR, see above) per 50 µl reaction volume containing $MgCl_2$ (2 mM, Invitrogen), dNTPs (each of 200 µM, Invitrogen), primer forward/reverse (750 nM, TIB Molbiol) and 1 U PlatinumTaq DNA polymerase in PCR buffer (Invitrogen) under the following conditions: 94 °C (5 min), 45 cycles 94 °C (30 s), 60 °C (30 s), 72 °C (2 min) and finally 72 °C (5 min).

2.5.3. Cycle-sequencing according to Sanger

Nested PCR products were first purified using an MSB®Spin PCRapace Kit (Invitek) and then sequenced using the BigDye®Terminator v3.1Cycle Sequencing Kit (Applied Biosystems) and a capillary sequencer 3130xl (Applied Biosystems). Trimming and reference mapping were done with Geneious software (11.1.5) and influenza A(H1N1) pdm09 HA and NA gene nucleotide sequences were deposited in GISAID.

2.5.4. Whole genome sequencing (WGS)

Prior WGS the One-Step RT-PCR products were purified using SPRIselect beads (Beckman Coulter) with a ratio of 0.6 according to the manufacturer (40 µl OneStepPCR product x 0.6 = 24 µl SPRIselect reagent). Then DNA quantification with Qubit dsDNA kit and a Qubit Fluorometer (ThermoFisher) was done. WGS was performed using 1 ng purified One-Step RT-PCR product, Nextera XT DNA Library Preparation Kit and subsequently the MiSeq platform (Illumina). Trimming, reference mapping and generate consensus sequences (threshold 95 %) were done with Geneious software (11.1.5) and influenza A(H1N1)pdm09 whole genome sequences (minority variants ≥10 %) were deposited in GISAID.

2.6. Phylogenetic analysis

Phylogenetic evaluation was done using Mega 7, neighbour-joining method, phylogeny test by bootstrap method and 1000 replications, Kimura 2 substitution model and partial deletion (site coverage cutoff 5 %). The viral sequences obtained from different anatomical sites of this single patient were compared with selected sequences of A(H1N1) pdm09 viruses collected during the National Influenza Centre's virological surveillance of seasons 2017/18 (n = 9, including described fatal case) and 2018/19 (n = 11).

2.7. Virus titration

Samples were titrated at lg dilutions in MDCK SIAT cells in microtiter plates (EMEM + 0.2 % Trypsin + 1 %l L-Glutamine + 0,5 % Gentamycin + 1 % NEAA) and incubated at 33 °C over 36 h. Then cells were fixed with 3.5 % Formalin at room temperature over 15 min. Afterwards

Triton X-100(Surfact-Amps X-100)/Thermo Scientific) was added and incubated at room temperature over 10 min. Afterwards cells were 3x washed using washing buffer (PBS + 0.05 % Tween 20). Then anti-Influenza A-NP-antibody HB65 (Clonegene) diluted 1:500 in blocking buffer (PBS + 30 % BSA+ 0.1 % Tween-20) was added. The reaction was incubated at 33 °C over 1 h and then plates were 3x washed using washing buffer. Afterwards goat anti-mouse IgG, HRP (Invitrogen) diluted 1:500 in blocking buffer was added and incubated at 33 °C over 1 h. After 3x washing with washing buffer, AEC (AEC 101 staining kit, Sigma Aldrich) was added according to the instructions of the manufacturer and incubated at room temperature over 1 h. Thereafter the microtiter plates were washed with aqua dest. Finally, the staining reaction was evaluated under light microscope. $TCID_{50}$ was calculated according to the method of Spearman & Kärber (Kärber, 1931; Spearman, 1908).

2.8. Antigenic analysis

The viruses were investigated for their antigenic properties by hemagglutination inhibition (HI) assay using antisera generated in ferrets against the vaccine strains of the influenza season 2017/18. HI assays were based on turkey and guinea pig red blood cells (the latter for H3N2). The viruses were adjusted to 8 hemagglutinating units for analysis. For ferret antisera generation, ferrets were infected intranasally with 10^5 $TCID_{50}$ of each vaccine strain and blood was sampled 14 days later.

2.9. Resistance analysis

Inhibition of viruses cultured from post-mortem nasal swab and one lung-biopsy sample by the neuraminidase inhibitors (NAI) oseltamivir and zanamivir was analyzed using a fluorometric neuraminidase inhibition assay with 2′-(4-Methylumbelliferyl)-a-D-N-acetylneuraminic acid (Munana) as substrate as described elsewhere (Duwe and Schweiger, 2008). Antiviral susceptibility of these viruses was assessed based on the fold-change of the IC_{50} value compared to reference IC_{50} values according WHO guidelines (WHO. Meetings of the WHO working group on surveillance of influenza antiviral susceptibility-Geneva, November 2011 and June 2012. Available from: http://www.who.int/wer/2012/wer8739.pdf.) Neuraminidase amino acid sequences were aligned with sequences of the respective reference vaccine strains and analyzed for molecular resistance markers associated with reduced NAI susceptibility.

2.10. Studies in porcine airway epithelial cells

2.10.1. Preparation of air-liquid interface cultures of porcine airway epithelial cells

Porcine lungs used in this study were obtained from a local slaughterhouse. Air-liquid interface (ALI) cultures of porcine airway epithelial cells were generated as previously described (Fulcher et al., 2005; Meng et al., 2016).

2.10.2. Virus infection

Well-differentiated porcine bronchial epithelial cells (PBEC) were 3x washed with phosphate-buffered saline (PBS) and then infected by either of the viruses from lower and upper respiratory tract of the fatal case at an infectious dose of 10^4 $TCID_{50}$ per filter in 100 µl ALI medium. After incubation at 37 °C for 1 h, the infectious medium was removed and cells were 3x washed with PBS to remove unbound virions. Finally, 600 µl ALI medium was added to the basal compartment to maintain the cells. To determine the virus release, 100 µl ALI medium was added at the respective time points to the apical compartment and incubated at 37 °C. After 30 min, the apical medium was collected and used to determine the viral infectivity by endpoint dilution titration on MDCK cells as described previously (Yang et al., 2017).

2.10.3. Detection of trans-epithelial electrical resistance (TEER)

The TEER developed by well-differentiated PBEC was measured before infection and for a period of eight days after infection by using the Millicell ERS-2 (Millipore) equipment. The apical and basal compartments of transwell filters were washed three times with PBS, then 200 µl PBS were added to the apical compartment and 500 µl PBS to the basal compartment. TEER was determined according to the manufacturer's instructions.

2.10.4. Immunofluorescence microscopy

All infected and mock-infected samples were 3x washed with PBS and fixed with 3 % paraformaldehyde (PFA) for 20 min. PFA was removed and 0.1 M glycine was added for 5 min. Samples were permeabilized with 0.2 % Triton X-100, 3x washed with PBS and treated with 1 % bovine serum albumin (BSA) for 30 min to block nonspecific binding sites. Primary and secondary antibodies were diluted with 1 % BSA in PBS and incubated with the samples for 1 h each. After washing with PBS, samples were incubated with DAPI (4′,6-diamidino-2-phenylindole) for 20 min. Finally, transwell filters were taken out by using a scalpel and embedded in Prolong Gold Antifade Reagent (Life Technologies), and stored at 4 °C for further analysis.

Antibodies against influenza A virus nucleoprotein (NP, 1:750, AbDSeroTec), against mucin-5 AC (1:250, Santa Cruz Biotechnology), against ZO-1(1:250, Life Technologies) and Cy3-labeled antibody against β-tubulin (1:500, Sigma) were used as primary antibodies. Green fluorescence and red fluorescence (Alexa Fluor® 488 and 568) conjugated antibodies (1:1000, Life Technologies) were used as secondary antibodies. Samples were analyzed by using an inverse immunofluorescence microscope Nikon Eclipse Ti-S (Nikon) and TCS SP5 confocal laser scanning microscope (Leica). Images were analyzed by using NIS-Elements Viewer 4.20 software (Nikon), LAS AF Lite sofware (Leica) and ImageJ/Fuji software.

All in vitro-experiments were performed at least three times and data were analyzed with Tukey multiple comparison test by using the GraphPad Prism 5 software. Results were shown as means with standard deviations. A p value of < 0.05 was considered significant.

3. Results

3.1. Clinical and pathology report

A patient (age group 5–15 years) with clinical and laboratory findings suggestive of hemolytic uremic syndrome (HUS), including emesis and progressive renal failure was admitted to the hospital and died 13 h later. In the late clinical course, the patient displayed acute respiratory distress syndrome. Oropharyngeal swab, blood and stool samples had been taken shortly after admission. Investigations for *Campylobacter spp.*, *Salmonella spp.*, *Shigella spp.*, EIEC, EHEC and EPEC had been negative. Blood smears showed fragmentocytes indicative for damaged red blood cells. Autopsy revealed severe bilateral hemorrhagic pneumonia. Lung weight was 2.5× higher than normal. At autopsy, lung specimens and pharyngeal, laryngeal and tracheal swabs were obtained. qPCR of the lung samples yielded strong signals for influenza A and subtype A(H1N1)pdm09.

3.2. qPCR, virus isolation, antigenic characterization and resistance analysis

qPCR analysis revealed the presence of A/H1N1)pdm09 virus in the entire respiratory tract (Table 1, Table S1). The respiratory panel multiplex (RT-)PCRs were negative for influenza B virus, respiratory syncytial virus, human metapneumovirus, human rhinovirus, human coronaviruses 229E, NL63, HKU1, OC43, parainfluenzavirus 1–4, bocavirus, parechovirus, enterovirus, adenovirus and *Mycoplasma pneumoniae*. Viruses were isolated from different anatomical sites in MDCK SIAT cells. On antigenic characterization, the isolates displayed

Table 1
Virological characterization of respiratory tract specimens from a fatal case of A(H1N1)pdm09 influenza.

Sample	Original material post-mortal	CT[1]	HI[2]	Amino acid substitutions[3,4]										
				HA[5]	M1	M2	NA[5]	NP	NEP	NS1[5]	PA[5]	PA-X[5]	PB1	PB2[5]
				HA1: S74R, P137S, S164T, S183P, R223Q, I295VHA2: N124T			G77R, V80M, V81A, I188T, N449D			M65V		R199K		R299K, T398I, P453T
SAL25 (1316)	lung biopsy left	33	2560	*S263*									*H456X-H/Y 98 %*	
SAL30 (1314)	lung swab left	31	nd	*K208X-K/N 15 %*			*S89X-S/T 11 %, S367X-S/L 11 %*				nd	nd	*H456X-H/Y 91 %*	
SAL28 (1311)	trachea	31	nd	*S263X-S/F 22 %*							nd	nd	*H456X-H/Y 34 %, V514X-V/A 16 %*	
SAL29 (1312)	larynx	33	nd	*S263X-S/F 31 %*							nd	nd	*H456X-H/Y 14 %*	*E305X-E/D 18 %*
SAL24 (1310)	nasal swab	27	2560	*S263X-S/F 22 %*							nd	nd	*H456X-H/Y 9 %*	
SAL25 MDCK	lung biopsy left	33	nd	*S263*									*H456Y*	
SAL24 MDCK	nasal swab	27	nd	*S263X-S/F 3 % decreased*									*H456X-H/Y 38 % increased*	

[1] CT, cycle threshold A(H1N1)pdm09-qPCR Berlin (for further details see supplemental data table S1).
[2] HI, reciprocal titer against A/Michigan/45/2015 A(H1N1)pdm09.
[3] Amino acid substitutions in the indicated genome region (column header), relative to A/Michigan/45/2015 A(H1N1)pdm09.
[4] *Italics* indicate minority variants as determined by NGS investigation. Shown are ≥ 10% minority variants in the deduced amino acid mixtures. For HA1-263 and PB1-456, also minority variants <10% are indicated. The proportion of substitutions relative to the reference sequence is shown in (%).
[5] This row lists substitutions common to all specimens.

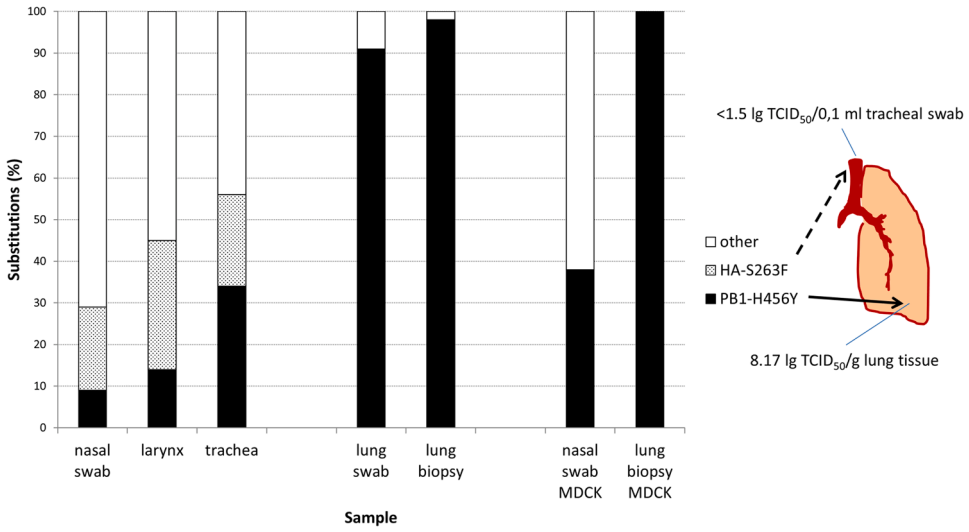

Fig. 1. Percentage of striking aa substitutions and viral load in upper and lower respiratory tract samples.
MDCK: analyses of isolates obtained from the corresponding tissue in MDCK-SIAT cells; other: indicates the proportion of the amino acid serine (S, HA1–263) or histidine (H, PB1–456) in each of the detected amino acid mixtures (HA1-S263S/F, PB1-H456H/Y).

strong reactivity with anti-A/Michigan/45/2015 A(H1N1)pdm09 ferret serum but not with sera against A(H3N2) and B viruses (Table 1, Table S1). The viruses were inhibited by oseltamivir and zanamivir with IC_{50} values similar to reference viruses; molecular resistance markers were not detected. Titration of virus of the respiratory tract samples in MDCK-SIAT cells demonstrated very high titers of infectious virus in the lung sample (8.17 lg $TCID_{50}$/g), but low titers of infectious virus in upper respiratory tract (Fig. 1, Table S1).

3.3. Sequence analysis of viral samples of the fatal case

In this fatal case of pediatric influenza in a hospitalized child with hemorrhagic pneumonia, viral HA sequence analyses in tissue samples from different sites in the upper and lower airways demonstrated that the A(H1N1)pdm09 virus belonged to the clade 6B.1 A. Whole genome analysis of the samples revealed the presence of a mixed genotype, both in the HA (S263S/F [HA1]) and the PB1 genes (H456H/Y [PB1]) at different proportions (relative to A/Michigan/45/2015): In the post-mortem nasal swab as well as larynx and trachea, a proportion of viruses (22–31 %) displayed the HA1 substitution S263F, which was not found in the lung, whereas in the lung, a major proportion (91–98 %) of viruses featured the PB1 substitution H456Y, which was only seen at low proportions in the upper respiratory tract with decreasing percentages from regions closer to the lung (trachea 34 %) to more distant regions (larynx 14 %, nasal swab 9 %) (Table 1).

3.4. Screening for substitutions HA1-S263F and PB1-H456Y in 2017/18, 2018/19, 2019/20 and 2022/23 influenza viruses

Among the 318 influenza A(H1N1)pdm09 viruses screened during the 2017/18, 2018/19, 2019/20 and 2022/23 seasons at the National Influenza Centre, the substitution S263F in HA1 was only found in this fatal case (fatal-1, Table 2). The H456Y polymorphism in PB1 was identified in two one-year-old children in January 2020 who were infected with clade 6B.1A5A viruses, one of them with fever (39 °C).

Table 2
Screening for HA-S263F, PB1-H456Y, PB1-H456H/Y substitutions in 2017–2023 A(H1N1)pdm09 influenza viruses.

Season	Number	HA-S263F	PB1-H456Y	PB1-H456H/Y
2017/18	57	1x (fatal-1)	1x (fatal-1)	1x (fatal-1)
2018/19	65	0	0	0
2019/20	141	0	2x (1-year-old)	0
2022/23	55	0	0	0

3.5. Comparative sequence analysis of HA

The genomes of A(H1N1)pdm09 viruses collected both in the 2017/18 (n = 9) and 2018/19 (n = 11) seasons were analyzed by whole genome sequencing via NGS and Sanger. In order to genetically compare viruses from patients with a severe course with viruses from outpatients, virus isolates from ten infants (1 - 4 y), four children (5 - 8 y) and six adults (26 - 64 y) were available from the sentinel surveillance. These viruses originated from three fatal cases (4 y, 5 y, 64 y), two severe cases (2 y, 37 y) and fifteen outpatients (14 sentinel and one non-sentinel). The HA gene analysis demonstrated that all viruses belonged to the clade 6B.1 A with the clade specific substitutions S74R, S164T and I295V in HA1 (relative to A/California/07/2009). Additionally, most of the analyzed viruses exhibited the substitution S183P in HA1, including the described fatal case (Fig. 2). The HA1 substitution S263F was not found in nasal swab samples except the case presented. Amino acid 263 is located between the globular head and the stem region of the hemagglutinin (Fig. 3). The analysis showed consistence between sequences characterized by NGS vs. those characterized by classical Sanger sequencing, with the only differences noted being due to the methodologies applied to determine minority variants: The detection limit for minority variants was about 20 % of the target reads using Sanger sequencing.

3.6. Comparative sequence analysis of PB1

The PB1 gene analysis demonstrated the presence of the substitutions G154D, I397M, I435T (relative to A/California/07/2009) in all analyzed viruses (Fig. 2). These substitutions were located in three of ten PB1 domains (fingers, ß-hairpin, palm). In 2018/19, a subgroup of viruses featured the additional substitutions V200I (ß-ribbon domain) and K386R (ß-hairpin domain) and two viruses displayed the D619G substitution (thumb domain). Furthermore, the H456Y and K430R substitutions, located in the palm domain of PB1 that contains the highly conserved catalytic site (D445, D446) of polymerase activity, were identified in viruses from both this fatal case (H456Y) and an outpatient (K430R), respectively (Fig. 3). Further virus-specific substitutions were identified in the fingers domain (T123A, D154G, N158S), ß-hairpin

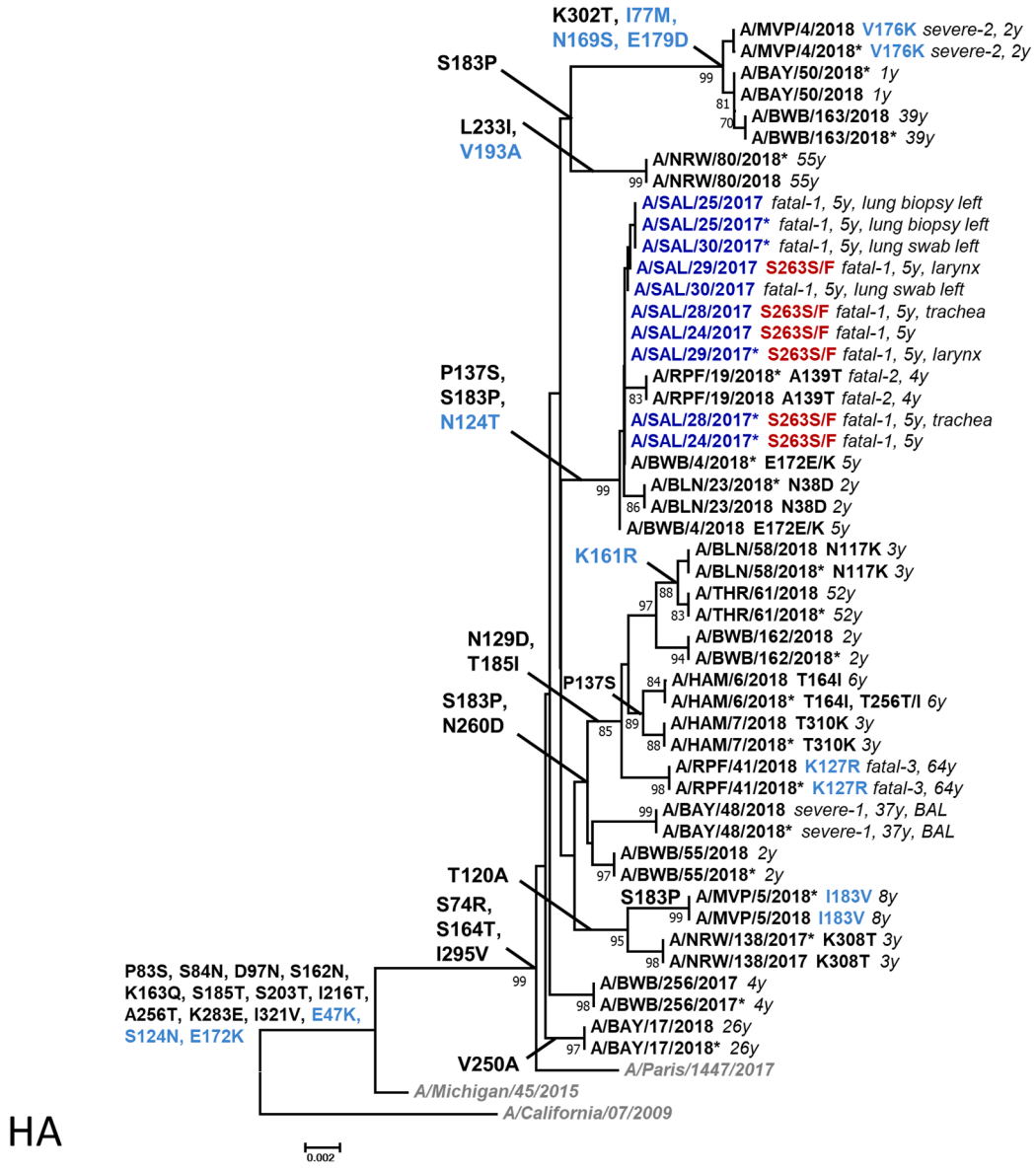

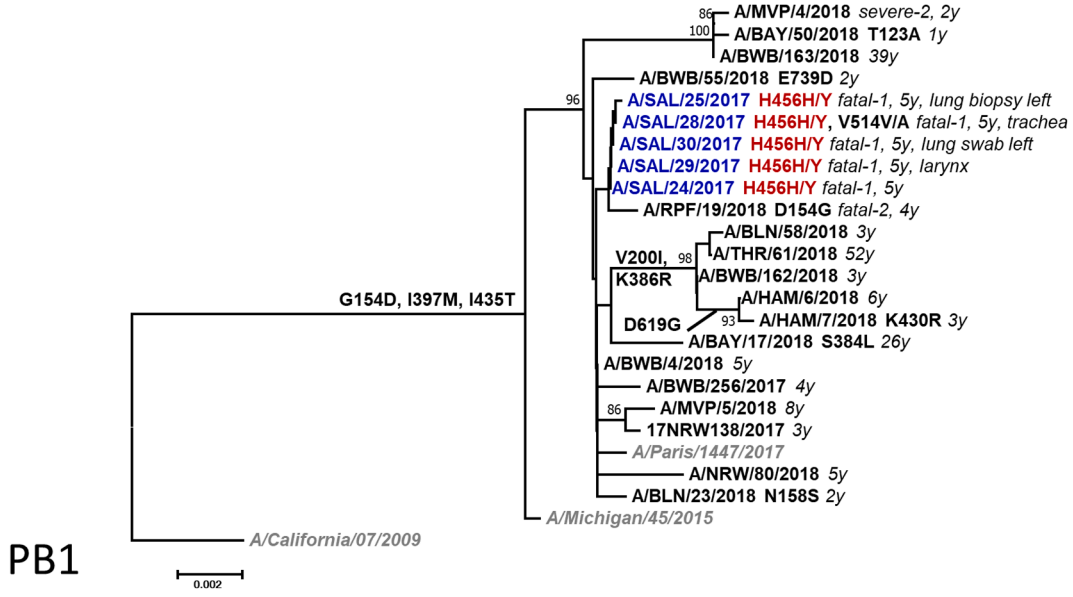

(caption on next page)

Fig. 2. Phylogenetic analysis of the HA and PB1.
The HA (n = 20) of and PB1 (n = 18) genes of A(H1N1)pdm09 viruses circulating in the 2017/18 (weeks 50/2017 – 13/2018) and in the beginning of the 2018/19 (weeks 44 – 52/2018) season were employed for phylogenetic analysis. Whole virus genomes were analyzed by NGS and HA genes were analyzed by Sanger sequencing (asterisk). Reference sequences of WHO are marked in grey/italics. Shown are phylogenetic analysis results of viruses from the described fatal case (fatal-1, blue) and two other patients with fatal outcome (fatal-2/3), two patients with severe course (severe-1/2), 14 sentinel outpatients and one non-sentinel outpatient. Unless otherwise indicated, the viruses were recovered from nasal swabs. Amino acid substitutions in HA1 (black)/HA2 (light blue) and aa mixes are indicated. The S263S/F (HA1) and H456H/Y (PB1) identified in fatal-1 specimens are labeled in red. Phylogenetic analysis was done with Mega7 (Neighbor-Joining method, bootstrap test with1000 replicates, Kimura 2-parameter method, partial deletion – site coverage cutoff 5 %).

domain (S384L) and the C-terminal domain (E739D) of PB1.

3.7. Virus replication kinetics in well-differentiated PBEC

To find out whether the viruses obtained from the upper and lower respiratory tract differed in their virulence properties, their replication in well-differentiated bronchial epithelial cells (PBEC) was analyzed. For this purpose, primary respiratory epithelial cells were cultured on filter supports under air-liquid interface (ALI) conditions until they were well-differentiated. Immunostaining indicated that the two viruses did not differ in the cell tropism. Ciliated cells identified by anti-tubulin antibodies were the major cell type infected as indicated by co-staining with anti-nucleoprotein antibodies (data not shown). Differences between the two viruses were revealed when the virus replication kinetics were determined: Well-differentiated PBEC were infected with either of the viruses and supernatants were collected at 16 h, 24 h, 48 h, 72 h, 96 h and 120 h post infection (p.i.) and the amount of infectious virus released at the respective time point was determined. The kinetics of virus release is shown in Fig. 4. Viruses from the lower respiratory tract grew faster and to higher titers than viruses from upper respiratory tract. At 24 h p.i. the differences were more than tenfold and highly significant (Fig. 4).

In mock-infected samples, the majority of cells were ciliated cells (Fig. 5a). This high proportion was slightly decreased in ALI cultures infected by viruses from the upper respiratory tract. A larger decrease was observed when well-differentiated PBEC were infected by viruses from the lower respiratory tract (Fig. 5a). Quantification of the area covered by cilia staining revealed a reduction of about 20 % between the

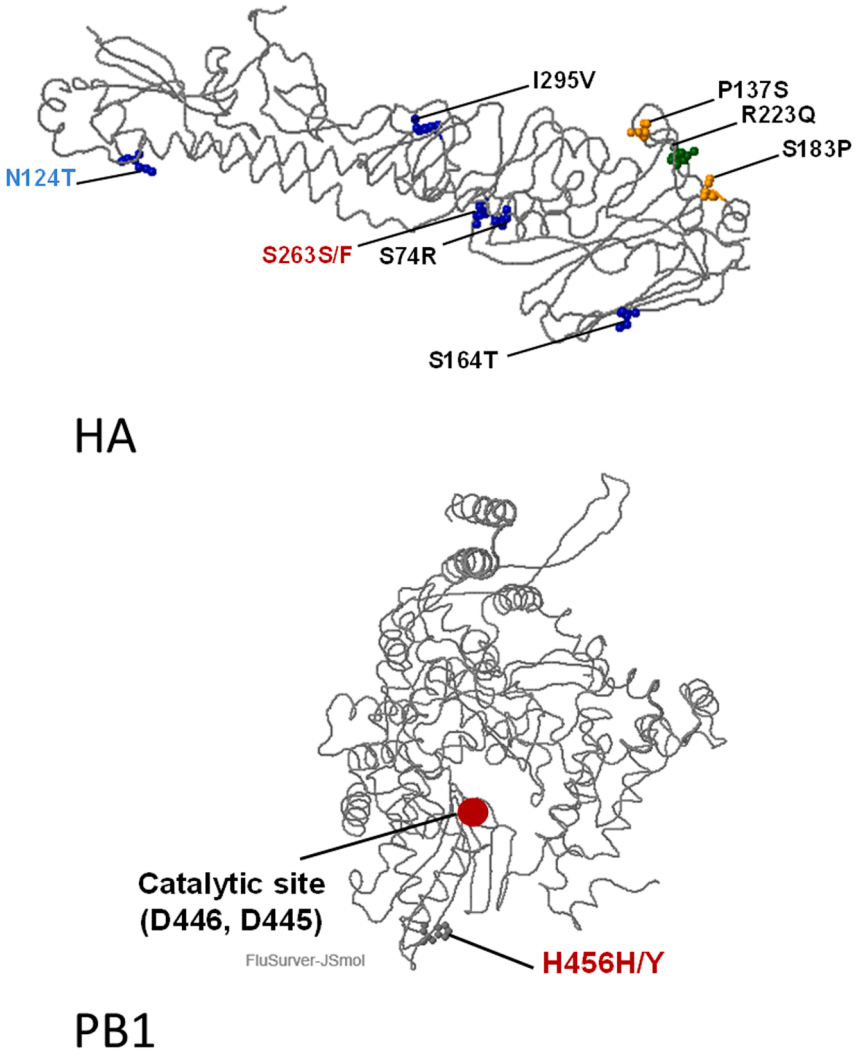

Fig. 3. 3D-model of sequence detected in fatal-1 specimens.
3D-models of HA and PB1 proteins of A(H1N1)pdm09 viruses detected in fatal-1 specimens were deduced by using https://flusurver.bii.a-star.edu.sg/ in order to assess the positions of the identified substitutions in the viral proteins relative to the reference strain A/Michigan/45/2015.

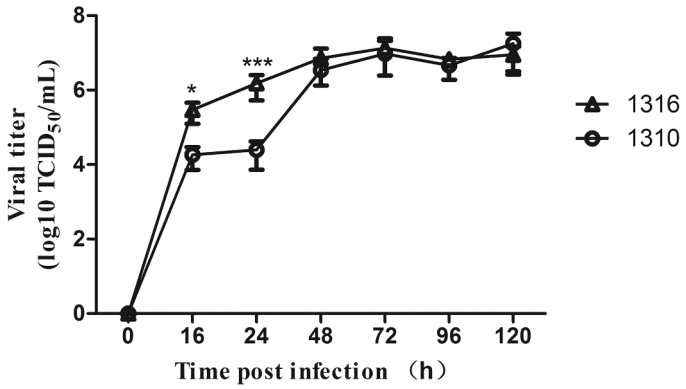

Fig. 4. Replication kinetics of viruses from lower (1316) and upper (1310) respiratory tract in PBEC.
PBEC cultures were apically infected with the viruses at infection dose of 10^4 $TCID_{50}$/filter, at 37 °C. After 1 h, samples were washed three times with PBS to remove free virions. Supernatants were collected at 16 h, 24 h, 48 h, 72 h, 96 h and 120 h post infection and analyzed for infectivity with $TCID_{50}$ assay. The results are shown as means ± SD of samples of three independent experiments, each with three replicates. Significance (*$P < 0.05$, ***$P < 0.001$) was analyzed with Tukey multiple comparison test by using the GraphPad Prism 5 software. Sequence data of supernatants were not established.

two viruses and the difference was significant (Fig. 5b).

Virulence-related differences in the loss of ciliated cells after infection by human or animal influenza A viruses have been reported before. The TEER values determined for PBEC infected by either of the two viruses from the upper and lower respiratory tract was also not reduced compared to mock-infected sample (not shown).

Taken together, infection of porcine ALI cultures by viruses from lower and upper respiratory tract of the fatal case resulted in (i) virus release over a long period of time and (ii) loss of ciliated cells. These effects were more pronounced in infections by lower respiratory tract virus than they were in cultures infected by upper respiratory tract virus.

4. Discussion

We investigated the unusual course of an influenza A virus infection caused by A(H1N1)pdm09 virus in a child. Respiratory symptoms were not obvious in the initial clinical presentation of this case, which was predominated by features of hemolytic uremic syndrome associated with gastrointestinal symptoms. Due to this atypical presentation, the association with influenza was not obvious. Acute respiratory distress syndrome evolved only in the final stage. At autopsy, the hemorrhagic changes in the entire lung suggested a potential infectious etiology and multiplex (RT-)PCR analysis of a pre-mortem oropharyngeal swab, as well as extensive post-mortem biopsy analyses, revealed an A(H1N1) pdm09 virus infection.

Whereas the lung specimen displayed a high load of infectious virus, infectivity of all other respiratory tract samples remained below the assay limit of detection. In line with these results, qRT-PCR testing of a pharyngeal swab sample obtained on admission revealed comparatively high Ct values (33 in influenza A-qPCR and >35 in A(H1N1)pdm09-qPCR), indicating low viral loads in the patients' upper respiratory tract.

The genomes of viruses from upper airway samples and lung displayed mixtures of S263S/F (HA1) and H456H/Y (PB1) variants. The amino acid substitution S263F in HA1 was only found in the post-mortem nasal swab, larynx and trachea, whereas in the lung samples, the PB1 substitution H456Y was predominant. Viruses from the lung tract had a replication advantage in vitro and grew faster to higher titers than the viruses of the upper respiratory tract. The patient's lung sample contained a high viral load of 8.17 lg $TCID_{50}$ per gram lung tissue. These very high amounts of viruses in the lung may explain the rapid progression of the disease. The lower respiratory tract of children provides a microenvironment supporting the replication of A(H1N1)pdm09 and some avian influenza viruses. Human lung type II pneumocytes possess SA(sialic acid)-α-2,3 receptors in addition to SA-α-2,6 receptors (Shinya et al., 2006), which allow for the specific binding of the hemagglutinin of influenza viruses (Kumlin et al., 2008) and support virus entry into lower respiratory tract cells in addition to other receptors (Ge and Wang, 2011). There are differences in the isoforms of lectin-binding to SA-α-2,3 receptors, which support stronger binding of influenza viruses to the epithelium of children than to adults (Nicholls et al., 2007), as well as of avian influenza (Matrosovich et al., 1999) and A(H1N1)pdm09 viruses (Childs et al., 2009). Severe and fatal influenza (as caused for example by A(H5N1) viruses) is frequently associated with a widespread distribution of influenza viral genetic information and/or its antigenic expression in different tissues of the body and the induction of a cytokine storm (Gu et al., 2007). There is a strong correlation between viral load and the induction of proinflammatory cytokines in patients with fatal outcome of influenza (De Jong et al., 2006). Severe A(H1N1) pdm09 influenza is commonly associated with increased levels of cytokines such as IL-6, IL-10, IL-15, IP-10, IL-2R, HGF, ST2, MIG and others (Bradley-Stewart et al., 2013; Martinez-Ocaña et al., 2013). Thus, it is possible that the lack of basal immunity against influenza viruses in children (because there was no contact to influenza viruses before), combined with the special features found in the developing lung, provide an environment conducive to the selection of quasispecies with

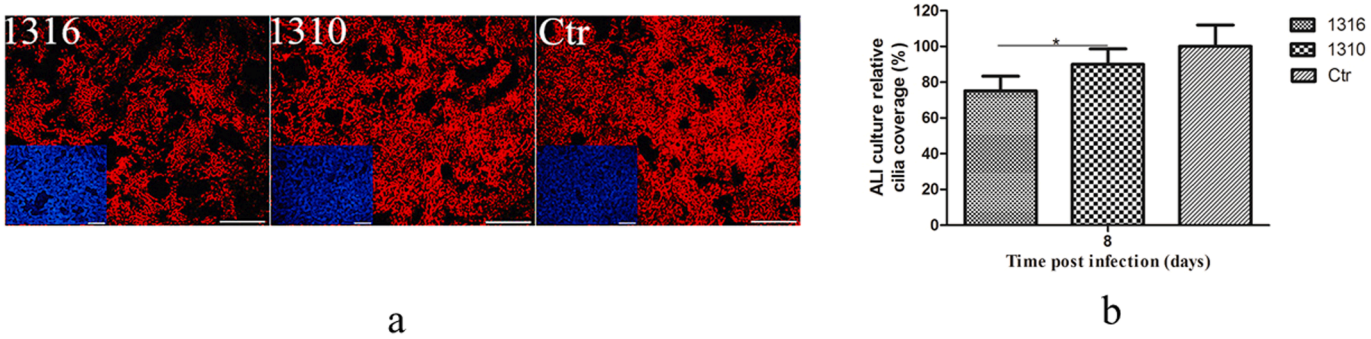

Fig. 5. Cilia coverage of PBEC on 8 d post infection.
PBEC cultures were apically infected with viruses from lower (1316) and upper (1310) respiratory tract at infection dose of 10^4 $TCID_{50}$/filter. (a) After 8 d post infection, PBEC cultures were stained with Cy3 labelled β-tubulin to detect cilia (red). Scale bar, 100 μm. (b) Quantitative analysis of area covered by cilia at 8 d post infection. The ALI culture relative cilia coverage (%) was shown as means ± SD compared to mock-infected cultures (Ctr). Nine samples from three independent experiments were determined, three fields from one sample were evaluated. Significance (*$P < 0.05$) was analyzed with Tukey multiple comparison test by using the GraphPad Prism 5 software.

enhanced replication properties that are particularly effective. Moreover, for A(H1N1)pdm09 viruses, several mutations have been previously identified that may be linked to increased virulence (Goka et al., 2014).

As virus isolated from the lung showed signs of increased virulence, we looked for hints supporting special properties of the respective mutations in the scientific literature. Specific A(H1N1)pdm09 virus variants replicating preferentially in the lower respiratory tract were also reported in Italy in the season 2010/11 (Piralla et al., 2011). One of the viruses had a D222G and S263F amino acid substitution in the hemagglutinin (HA1) and the infection led to a fatal outcome (Piralla et al., 2011). A mouse-adapted swine influenza A(H6N6) virus had an alteration at position 263 of the hemagglutinin (HA1) and showed enhanced virulence in mice (Tan et al., 2014). A mutation at position 263 of the HA1 in A(H5N1) viruses influenced the conformational stability of HA, increased the resistance to stem mAbs, facilitated the formation of escape mutants and conferred a modest but significant increase in both the thermal stability and pH stability of the hemagglutinin (Wang et al., 2018). The acid stability of the hemagglutinin varies among influenza viruses and is a factor affecting infectivity and adaptation to host cells. The pH value gradually increases from the human upper to the lower respiratory tract. The hemagglutinins of A(H1N1)pdm09 viruses have been reported to be less pH-stable than other seasonal influenza A viruses (Long et al., 2019; Wang et al., 2015). Located between the globular head and the stem region of the hemagglutinin, the amino acid 263 is in a region that undergoes changes in secondary and tertiary structure during protein folding (Russell, 2021). The change at position 263 may very well represent a local adaptation of the virus to an altered microenvironment resulting in altered replication efficiency.

Important processes for regulating the pH value of body fluids are buffering, regulation through breathing (removal of CO_2) and regulation through the kidneys or metabolism. A significant interaction between kidneys and lungs has been shown in physiological and pathological conditions in which the two organs can both be targets of the same systemic disease (e.g., some vasculitides). Moreover, loss of normal function of either of them can induce direct and indirect dysregulation of the other one (Sorino et al., 2019). In the case of acute lung diseases (e.g. hemorrhagic pneumonia) and / or kidney failure (e.g. HUS), the regulation of the pH value can be disturbed in the different organs (Fajardo-Dolci et al., 2010).

Another mutation HA1-S183P was found in the majority of A(H1N1)pdm09 viruses, which circulated during the seasons under investigation. The virus of the investigated case shares this mutation. HA1-S183P A(H1N1)pdm09 variants of human lung cell cultures showed significantly increased binding to several α2,6 SA-linked glycans (Lee et al., 2018), which might result in a tropism alteration.

The PB1-H456Y substitution, which was found in the fatal case investigated here, is located near the PB1 catalytic site (D445, D446) (Fan et al., 2019). This PB1-H456Y polymorphism was previously linked with increased virulence in a mouse infection model (Hiromoto et al., 2000) and – in a similar way - may have enhanced local virus replication in the lung thereby contributing to the severe disease of the child.

When comparing A(H1N1)pdm09 viruses isolated from nasal swabs of outpatients and hospitalized patients in Germany, we found that the HA1-S263F mutation was unique and has not been detected in other specimens of the corresponding season (2017/18) and the following seasons (2018/19, 2019/20, 2022/23); the PB1-H456Y substitution was only found in two sentinel specimens of another season (2019/20), both viruses being derived from one-year old children.

Also in another study investigating nine ICU patients with A(H1N1)pdm09 infection neither HAI-S263F nor PB1-H456Y mutations were found (Takayama et al., 2021). Given that the difference between samples of the lung and upper respiratory tract was most likely pathogenetically relevant it is worth to consider a specific focus on lower respiratory tract samples (BAL, lung tissue) in routine influenza surveillance.

We have recently shown that human A(H1N1)pdm09 viruses in the years following the 2009 pandemic have evolved toward lower virulence (Fu et al., 2019). Viruses isolated from human patients in 2009 caused lethal illness in pigs and induced a remarkable loss of ciliated cells in the in vitro system, whereas less virulent viruses isolated after 2009/2010 did not. The investigation of viruses from the fatal human case described here did not induce such a pronounced loss of ciliated cells as induced by the above mentioned highly virulent virus of 2009 but the PB1-H456Y virus obtained from the lung of the fatal case replicated faster and caused a larger reduction in the number of ciliated cells in vitro compared to virus isolated from the upper respiratory airways of the same case. A likely explanation is that the virus has evolved locally to achieve high replication fitness in the lower respiratory tract. Individual host factors may have been a major contributor to the fatal outcome: i) by providing a microenvironment facilitating the evolution of a virus with extremely high replication competence and ii) via the individual proinflammatory immune response (Weinheimer et al., 2012). It should be noted that the loss of ciliated cells does not affect the barrier function of the epithelium as basal cells fill the gap and start to differentiate. This is evident from the fact the transepithelial resistance (TEER) is not reduced, even after infection by a virulent virus such as the A(H1N1)pdm09 virus.

The adverse outcome of influenza in immunologically naïve infants may be caused by an enhanced replication of viruses in their lower airways. After local evolution of highly virulent virus variants, the host may be overwhelmed by a fulminant hyperinflammatory reaction in the lung, which is associated with a general dissemination of viral genes and proteins and unusual disease patterns involving inflammation in organs other than the respiratory tract. Although the PB1-H456Y viruses were sensitive to neuraminidase inhibitors, it was not possible to provide antiviral treatment to this patient due to the unusual and rapid course of the disease. Given that the viruses were covered by the seasonal influenza vaccine, vaccination could have been advantageous. Vaccination against influenza is important for individual protection. Although vaccination cannot permanently prevent infection, it provides a rapid immune response to infection that prevents viral replication to high titers, thereby reducing symptoms and preventing fatal disease. In addition, vaccination can help achieve herd immunity when administered simultaneously to large groups. In this case, vaccination contributes significantly to preventing high viral loads in the environment, reducing the risk of infection and, if infected, the risk of severe outcomes. This is particularly important for children, as most of them have not been exposed to viral antigens and the congregation in kindergartens and schools supports the transmission and accumulation of viruses in aerosols.

5. Conclusions

In conclusion, the wild-type and two variants of influenza A(H1N1)pdm09 viruses circulating in the 2017/18 season were detected in the post-mortem respiratory specimens from upper respiratory tract and lung in a fatal case. The HA1–263F variant was only detected in the nasal sample, larynx and trachea, which may be associated with increased pH stability and reduced conformational flexibility of the hemagglutinin in comparison to the HA1–263S wild type. On the other hand, the PB1–456Y variant was identified primarily in the lung samples, which was associated with faster in vitro replication of the virus compared to the PB1–456H wild type.

Influenza virus quasispecies may differ gradually between upper and lower respiratory tract, which may be due to different conditions in anatomic areas. This is of importance when sequences of influenza viruses obtained from the upper respiratory tract are used to analyze markers of virulence. In such cases the additional investigation of bronchoalveolar lavages or lung tissue specimens is recommended.

Dedication

This work is dedicated to Prof Dr Martin Mielke. Prof Dr Mielke supported our work over all the years with a great deal of commitment and empathy. We are indebted to him for his valuable advice and support at all times.

Funding

The work of GH was supported by grants from the Deutsche Forschungsgemeinschaft, Germany (DFG): [He1168/15-1; He1168/19-1]. The work of TW was supported by Bundesministerium für Bildung und Forschung, Germany (BMBF): [project "RAPID 01KI1723F"]. The funders had no role in study design, data collection and analysis, decision to publish, or preparation of the manuscript.

CRediT authorship contribution statement

Marianne Wedde: Investigation, Methodology, Visualization, Writing – review & editing, Data curation, Writing – original draft. **Barbara Biere:** Data curation, Investigation, Writing – review & editing, Methodology. **Yuguang Fu:** Investigation, Visualization, Methodology, Writing – review & editing. **Susanne Duwe:** Investigation, Methodology, Writing – review & editing. **Andrea Thürmer:** Investigation, Writing – review & editing. **Rainer M. Bohle:** Investigation, Writing – review & editing. **Fidelis A. Flockerzi:** Investigation, Writing – review & editing. **Ralf Dürrwald:** Conceptualization, Data curation, Investigation, Methodology, Visualization, Writing – original draft, Writing – review & editing. **Michael Zemlin:** Data curation, Investigation, Writing – original draft, Writing – review & editing. **Georg Herrler:** Funding acquisition, Supervision, Writing – original draft, Writing – review & editing, Methodology, Resources. **Jürgen Rissland:** Investigation, Writing – review & editing. **Thorsten Wolff:** Funding acquisition, Supervision, Writing – review & editing, Resources. **Thorsten Pfuhl:** Investigation, Writing – review & editing. **Christin Mache:** Investigation, Methodology. **Djin-Ye Oh:** Writing – review & editing, Writing – original draft. **Brunhilde Schweiger:** Methodology, Supervision, Writing – review & editing. **Sigrun Smola:** Investigation, Writing – review & editing, Data curation. **Janine Reiche:** Investigation, Writing – review & editing.

Declaration of Competing Interest

All authors declare no conflict of interest.

Acknowledgements

We thank Mareen Adam, Heike Fischer, Susi Hafemann, Ute Hopf-Guevara, Carmen Karstädt-Schulze, Katja-Irena Madaj, Jeanette Milde, Bettina Mischke, Christine Spingies, Anneliese Schindel, Maria Smallfield, Birgit Troschke, Nathalie Tollard, Robert Koch Institute, Berlin, Germany and Helga Appel, Institute of Virology, Saarland University Medical Center, Germany, for technical assistance, and Prof. Dr. Timm Harder, Friedrich-Loeffler-Institute, Isle of Riems, Greifswald, Germany for establishment of ferret antisera. Oseltamivir carboxylate and zanamivir were kindly provided out of charge for susceptibility testing by Hoffmann-La Roche Ltd and Glaxo Smith Kline GmbH & Co KG, respectively.

Appendix A. Supporting information

Supplementary data associated with this article can be found in the online version at doi:10.1016/j.ijmm.2024.151598.

References

Altmann, M., Fiebig, L., Buda, S., Von Kries, R., Dehnert, M., Haas, W., 2012. Unchanged severity of influenza A (H1N1) pdm09 infection in children during first postpandemic season. Emerg. Infect. Dis. 18, 1755.

Bradley-Stewart, A., Jolly, L., Adamson, W., Gunson, R., Frew-Gillespie, C., Templeton, K., Aitken, C., Carman, W., Cameron, S., McSharry, C., 2013. Cytokine responses in patients with mild or severe influenza A (H1N1) pdm09. J. Clin. Virol. 58, 100–107.

Childs, R.A., Palma, A.S., Wharton, S., Matrosovich, T., Liu, Y., Chai, W., Campanero-Rhodes, M.A., Zhang, Y., Eickmann, M., Kiso, M., 2009. Receptor-binding specificity of pandemic influenza A (H1N1) 2009 virus determined by carbohydrate microarray. Nat. Biotechnol. 27, 797–799.

Dawood, F.S., Iuliano, A.D., Reed, C., Meltzer, M.I., Shay, D.K., Cheng, P.-Y., Bandaranayake, D., Breiman, R.F., Brooks, W.A., Buchy, P., 2012. Estimated global mortality associated with the first 12 months of 2009 pandemic influenza A H1N1 virus circulation: a modelling study. Lancet Infect. Dis. 12, 687–695.

De Jong, M.D., Simmons, C.P., Thanh, T.T., Hien, V.M., Smith, G.J., Chau, T.N.B., Hoang, D.M., Van Vinh Chau, N., Khanh, T.H., Dong, V.C., 2006. Fatal outcome of human influenza A (H5N1) is associated with high viral load and hypercytokinemia. Nat. Med. 12, 1203–1207.

Duwe, S., Schweiger, B., 2008. A new and rapid genotypic assay for the detection of neuraminidase inhibitor resistant influenza A viruses of subtype H1N1, H3N2, and H5N1. J. Virol. Methods 153, 134–141.

Fajardo-Dolci, G., Gutierrez-Vega, R., Arboleya-Casanova, H., Villalobos, A., Wilson, K.S., Garcia, S.G., Sotelo, J., Cordova Villalobos, J.A., Diaz-Olavarrieta, C., 2010. Clinical characteristics of fatalities due to influenza A (H1N1) virus in Mexico. Thorax 65, 505–509. https://doi.org/10.1136/thx.2009.126953.

Fan, H., Walker, A.P., Carrique, L., Keown, J.R., Serna Martin, I., Karia, D., Sharps, J., Hengrung, N., Pardon, E., Steyaert, J., et al., 2019. Structures of influenza A virus RNA polymerase offer insight into viral genome replication. Nature 573, 287–290. https://doi.org/10.1038/s41586-019-1530-7.

Fu, Y., Dürrwald, R., Meng, F., Tong, J., Wu, N.H., Su, A., Yin, X., Haas, L., Schmidtke, M., Zell, R., et al., 2019. Infection STudies in Pigs and Porcine Airway Epithelial Cells Reveal an Evolution of A(H1N1)pdm09 Influenza A viruses toward lower virulence. J. Infect. Dis. 219, 1596–1604. https://doi.org/10.1093/infdis/jiy719.

Fulcher, M.L., Gabriel, S., Burns, K.A., Yankaskas, J.R., Randell, S.H., 2005. Well-differentiated human airway epithelial cell cultures. In: Human Cell Culture Protocols. Springer, pp. 183–206.

Ge, S., Wang, Z., 2011. An overview of influenza A virus receptors. Crit. Rev. Microbiol. 37, 157–165.

Girard, M.P., Tam, J.S., Assossou, O.M., Kieny, M.P., 2010. The 2009 A (H1N1) influenza virus pandemic: A review. Vaccine 28, 4895–4902.

Goka, E.A., Vallely, P.J., Mutton, K.J., Klapper, P.E., 2014. Mutations associated with severity of the pandemic influenza A(H1N1)pdm09 in humans: a systematic review and meta-analysis of epidemiological evidence. Arch. Virol.

Gu, J., Xie, Z., Gao, Z., Liu, J., Korteweg, C., Ye, J., Lau, L.T., Lu, J., Gao, Z., Zhang, B., 2007. H5N1 infection of the respiratory tract and beyond: a molecular pathology study. Lancet 370, 1137–1145.

Hiromoto, Y., Saito, T., Lindstrom, S., Nerome, K., 2000. Characterization of low virulent strains of highly pathogenic A/Hong Kong/156/97 (H5N1) virus in mice after passage in embryonated hens' eggs. Virology 272, 429–437. https://doi.org/10.1006/viro.2000.0371.

Kärber, G., 1931. Beitrag zur kollektiven Behandlung pharmakologischer Reihenversuche. Naunyn-Schmiede Arch. für Exp. Pathol. und Pharmakol. 162, 480–483.

Kumlin, U., Olofsson, S., Dimock, K., Arnberg, N., 2008. Sialic acid tissue distribution and influenza virus tropism. Influenza Other Respir. Virus 2, 147–154.

Lee, N., Khalenkov, A.M., Lugovtsev, V.Y., Ireland, D.D., Samsonova, A.P., Bovin, N.V., Donnelly, R.P., Ilyushina, N.A., 2018. The use of plant lectins to regulate H1N1 influenza A virus receptor binding activity. PLoS One 13, e0195525. https://doi.org/10.1371/journal.pone.0195525.

Long, J.S., Mistry, B., Haslam, S.M., Barclay, W.S., 2019. Host and viral determinants of influenza A virus species specificity. Nat. Rev. Microbiol 17, 67–81. https://doi.org/10.1038/s41579-018-0115-z.

Martinez-Ocaña, J., Olivo-Diaz, A., Salazar-Dominguez, T., Reyes-Gordillo, J., Tapia-Aquino, C., Martínez-Hernández, F., Manjarrez, M.E., Antonio-Martinez, M., Contreras-Molina, A., Figueroa-Moreno, R., 2013. Plasma cytokine levels and cytokine gene polymorphisms in Mexican patients during the influenza pandemic A (H1N1) pdm09. J. Clin. Virol. 58, 108–113.

Matrosovich, M., Matrosovich, T., Carr, J., Roberts, N.A., Klenk, H.-D., 2003. Overexpression of the α-2, 6-sialyltransferase in MDCK cells increases influenza virus sensitivity to neuraminidase inhibitors. J. Virol. 77, 8418–8425.

Matrosovich, M., Zhou, N., Kawaoka, Y., Webster, R., 1999. The surface glycoproteins of H5 influenza viruses isolated from humans, chickens, and wild aquatic birds have distinguishable properties. J. Virol. 73, 1146–1155.

Mena, I., Nelson, M.I., Quezada-Monroy, F., Dutta, J., Cortes-Fernández, R., Lara-Puente, J.H., Castro-Peralta, F., Cunha, L.F., Trovão, N.S., Lozano-Dubernard, B., 2016. Origins of the 2009 H1N1 influenza pandemic in swine in Mexico. Elife 5, e16777.

Meng, F., Wu, N.-H., Seitz, M., Herrler, G., Valentin-Weigand, P., 2016. Efficient suilysin-mediated invasion and apoptosis in porcine respiratory epithelial cells after streptococcal infection under air-liquid interface conditions. Sci. Rep. 6 (1), 13.

Nicholls, J.M., Bourne, A.J., Chen, H., Guan, Y., Peiris, J., 2007. Sialic acid receptor detection in the human respiratory tract: evidence for widespread distribution of potential binding sites for human and avian influenza viruses. Respir. Res. 8 (1), 10.

Piralla, A., Pariani, E., Rovida, F., Campanini, G., Muzzi, A., Emmi, V., Iotti, G.A., Pesenti, A., Conaldi, P.G., Zanetti, A., et al., 2011. Segregation of virulent influenza A(H1N1) variants in the lower respiratory tract of critically ill patients during the 2010-2011 seasonal epidemic. PLoS One 6, e28332. https://doi.org/10.1371/journal.pone.0028332.

Rath, B., Chen, X., Spies, V., Muehlhans, S., Obermeier, P., Tief, F., Seeber, L., Karsch, K., Milde, J., Skopnik, H., 2017. Prospective surveillance of antiviral resistance in hospitalized infants less than 12 months of age with A (H3N2) influenza infection and treated with oseltamivir. Antivir. Ther. 22, 515–522.

Russell, C.J., 2021. Hemagglutinin stability and its impact on influenza A virus infectivity, pathogenicity, and transmissibility in avians, mice, swine, seals, ferrets, and humans. Viruses 13. https://doi.org/10.3390/v13050746.

Shinya, K., Ebina, M., Yamada, S., Ono, M., Kasai, N., Kawaoka, Y., 2006. Avian flu: influenza virus receptors in the human airway. Nature 4, 321–326.

Skowronski, D.M., Leir, S., De Serres, G., Murti, M., Dickinson, J.A., Winter, A.-L., Olsha, R., Croxen, M.A., Drews, S.J., Charest, H., 2019. Children under 10 years of age were more affected by the 2018/19 influenza A (H1N1) pdm09 epidemic in Canada:↱ possible cohort effect following the 2009 influenza pandemic. Eurosurveillance 24, 1900104.

Sorino, C., Scichilone, N., Pedone, C., Negri, S., Visca, D., Spanevello, A., 2019. When kidneys and lungs suffer together. J. Nephrol. 32, 699–707. https://doi.org/10.1007/s40620-018-00563-1.

Spearman, C., 1908. The method of right and wrong cases (constant stimuli) without Gauss's formulae. Br. J. Psychol. 2, 227.

Streng, A., Prifert, C., Weissbrich, B., Liese, J.G., 2015. Continued high incidence of children with severe influenza A (H1N1) pdm09 admitted to paediatric intensive care units in Germany during the first three post-pandemic influenza seasons, 2010/11–2012/13. BMC Infect. Dis. 15 (1), 12.

Takayama, I., Nguyen, B.G., Dao, C.X., Pham, T.T., Dang, T.Q., Truong, P.T., Do, T.V., Pham, T.T.P., Fujisaki, S., Odagiri, T., et al., 2021. Next-generation sequencing analysis of the within-host genetic diversity of influenza A(H1N1)pdm09 viruses in the upper and lower respiratory tracts of patients with severe influenza. mSphere 6. https://doi.org/10.1128/mSphere.01043-20.

Tan, L., Su, S., Smith, D.K., He, S., Zheng, Y., Shao, Z., Ma, J., Zhu, H., Zhang, G., 2014. A combination of HA and PA mutations enhances virulence in a mouse-adapted H6N6 influenza A virus. J. Virol. 88, 14116–14125. https://doi.org/10.1128/JVI.01736-14.

Wang, W., DeFeo, C.J., Alvarado-Facundo, E., Vassell, R., Weiss, C.D., 2015. Intermonomer interactions in hemagglutinin subunits HA1 and HA2 affecting hemagglutinin stability and influenza virus infectivity. J. Virol. 89, 10602–10611. https://doi.org/10.1128/JVI.00939-15.

Wang, W., Song, H.S., Keller, P.W., Alvarado-Facundo, E., Vassell, R., Weiss, C.D., 2018. Conformational stability of the hemagglutinin of H5N1 influenza A viruses influences susceptibility to broadly neutralizing stem antibodies. J. Virol. 92 https://doi.org/10.1128/JVI.00247-18.

Weinheimer, V.K., Becher, A., Tonnies, M., Holland, G., Knepper, J., Bauer, T.T., Schneider, P., Neudecker, J., Ruckert, J.C., Szymanski, K., et al., 2012. Influenza A viruses target type II pneumocytes in the human lung. J. Infect. Dis. 206, 1685–1694. https://doi.org/10.1093/infdis/jis455.

Yang, W., Punyadarsaniya, D., Lambertz, R., Lee, D., Liang, C., Höper, D., Leist, S., Hernández-Cáceres, A., Stech, J., Beer, M., 2017. Mutations during the adaptation of H9N2 avian influenza virus to the respiratory epithelium of pigs enhance sialic acid binding activity and virulence in mice. J. Virol. 91, e02125–02116.

Zhou, B., Donnelly, M.E., Scholes, D.T., St. George, K., Hatta, M., Kawaoka, Y., Wentworth, D.E., 2009. Single-reaction genomic amplification accelerates sequencing and vaccine production for classical and Swine origin human influenza a viruses. J. Virol. 83, 10309–10313.